UNCOOLED THERMOPILE INFRARED DETECTOR LINEAR ARRAYS WITH DEFECTIVITY GREATER THAN 10^9 cmHz$^{1/2}$/W

Marc C. Foote, Eric W. Jones, and Thierry Caillat

Center for Space Microelectronics Technology

Jet Propulsion Laboratory

California Institute of Technology

Pasadena, CA 91109-8099

Keywords: Thermoelectric materials/devices, Infrared detectors, Microelectromechanical devices, Detectors, Noise measurement, Arrays

ABSTRACT

We have fabricated 63-element linear arrays of rnicromachined thermopile infrared detectors on silicon substrates. Each detector consists of a suspended silicon nitride membrane with 11 thermocouples of sputtered Bi-Te and Bi-Sb-Te films. At room temperature these detectors exhibit response times of 99 ms, zero frequency D^* values of 1.4x109 cmHz$^{1/2}$/W and responsivity values of 1100 V/W when viewing a 1000 K blackbody source. The only measured source of noise above 20 mHz is Johnson noise from the detector resistance. These results represent the best performance reported to date for an array of thermopile detectors. A test procedure is described that measures many of the relevant electrical, optical, and thermal properties of the detectors without specialized test structures.

Corresponding author: Marc C. Foote, MS 302-231, Jet Propulsion Laboratory, 4800 Oak Grove Drive, Pasadena, CA 91109, (8 18) 354-9009, FAX (8 18) 393-4540, email mare.c.footc@~jpl.nasa.gov

This work was sponsored by the National Aeronautics and Space Administration, Office of Space Science.

I. INTRODUCTION

The development of uncooled staring two-dimensional arrays of both resistive bolometers [1] and ferroelectric detectors [2] has shown the potential for uncooled thermal infrared detectors. A third class of thermal detectors, thermopiles, has not been developed in array formats to the extent of bolometers and ferroelectrics. However, these detectors are ideal for some applications due to simplicity in their system requirements. Thermopiles typically operate over a broad temperature range and are insensitive to drifts in substrate temperature. They are passive devices, generating a voltage output without bias or chopping. Thus, for some applications thermopile detectors can be supported by simpler, lower power, more reliable systems than either bolometers, pyroelectric or ferroelectric detectors. If thermopiles are read out with high-input-impedance amplifiers they exhibit negligible excess (l/f) noise since there is no current flow. They typically have high linearity over many orders of magnitude in incident infrared power.

A few groups have demonstrated micromachined arrays of thermopile infrared detectors. Several efforts have focused on silicon-based thermocouple elements, including polysilicon/gold [3,4], silicon/aluminum [5], and n-polysilicon/p-poly silicon [6]. All are linear arrays except a 128x 128 array of polysilicon thermopile detectors made by the Japan Defense Agency and NEC Corporation [6]. A major advantage of using silicon-based materials is that many of the processing steps can be done on a standard CMOS fabrication line, substantially reducing the cost for mass production. Properly doped silicon or polysilicon can have a Seebeck coefficient as large as 1 mV/K [6,7], resulting in a relatively large detector responsivity and facilitating low noise readout design. The Seebeck coefficient of polysilicon from typical CMOS fabrication facilities, however, is only about 100 μV/K [8,9]. A drawback of silicon or polysilicon as thermoelectric elements is that their thermoelectric figure of merit, Z, defined as the Seebeck coefficient squared divided by both the thermal conductivity and the electrical resistivity, is relatively low (Z= 1-4x10-5 K-') [10]. The defectivity of a thermoelectric detector increases roughly as the square root of Z [11]. Current silicon and polysilicon thermopile detector arrays have specific defectivity (D*) values less than 10* cmHz$^{1/2}$/W for 10 ms response times.

Honeywell has developed 128-element linear arrays of thermopile detectors using metal film thermoelectric [12, 13]. Metals such as constantan and chromel have a higher thermoelectric figure of merit than silicon or polysilicon ($Z \approx 10^{-4}$ K-'), but are not standard materials in CMOS fabrication lines. The Honeywell arrays have zero frequency D^* values of 1.4 x108 cmHz $^{1/2}$/W and 12 ms response times [14].

The materials with the highest thermoelectric figure of merit at room temperature are compounds in the $(Bi_{1-x}Sb_x)_2(Te_{1-y}Se_y)_3$ family. These materials can be difficult to fabricate in thin film form, but have the potential for the most sensitive detectors. Thermocouple detectors made with bulk $(Bi_{1-x}Sb_x)_2(Te_{1-y}Se_y)_3$ materials have demonstrated D^* values of 3-4 x109 cmHz 'n/W for a thermal response time of about 25 ms [15,16]. However, such detectors are hand assembled, difficult to make into arrays, fragile, and have low responsivity. Arrays of thin film $(Bi_{1-x}Sb_x)_2(Te_{1-y}Se_y)_3$ detectors have not been reported, but Völklein et al. report single thin film thermopile detectors with D^*=7.7x 10^8 cmHz$^{1/2}$/W and response times of 44 ms [17].

We report here the highest performance to date for arrays of thermopile detectors. Micromachined 63-element linear arrays exhibit D^* values of 1.4x109 cmHz$^{1/2}$/W and 99 ms response times. When performance is compared in a manner which takes into account differences in response time, this result represents an improvement in performance by a factor of 3.5 over other reported thermopile arrays. The arrays are composed of Bi-Te and Bi-Sb-Te thermoelectric lines on thermally isolated silicon nitride membranes with a silicon substrate. The pixels are 1.5 mm long with a 75 μm pixel pitch, matching the geometry of a compact spectrometer under development at Ion Optics, Inc. [18] Thermopile linear arrays such as these are well suited for compact, low power spectrometers because of their minimal system requirements and high broad-band D^* values.

II. DETECTOR FABRICATION

The Bi-Te and Bi-Sb-Te films were sputter deposited from a Kurt J. Lesker Torus 2 sputter gun [19]. A two inch diameter sputter target of composition $Bi_{0.4}Sb_{1.6}Te_{3.0}$ was purchased from Target Materials, Inc. [20] A second two inch target of composition $Bi_{2.0}Te_{3.5}$ was manufactured at

JPL. The $Bi_{20}Te_{35}$ target was made by mixing bismuth and tellurium shot, then annealing at about 650 “C in a sealed, evacuated quartz ampoule for 10 h. The ampoule was quenched in water, then the ingot was ground into a powder. The powder was pressed for 2 h at 350 “C with a pressure of about $8x10^{7}$ Pa. Films were deposited in a vacuum chamber with an initial pressure of about 10^{-4} Pa. An adhesion layer of titanium was thermally evaporated from a 75% tantalum, 25% titanium alloy wire [21]. This titanium adhesion layer dramatically y improved film adhesion without adversely affecting thermoelectric properties. Then a 1 μm thick Bi-Te or Bi-Sb-Te film was deposited with 0.7 Pa of argon gas, at ambient temperature, and with a target-substrate distance of 15 cm. In order to measure stress, Bi-Te and Bi-Sb-Te films were deposited on silicon nitride membranes designed to deform under stress. Little or no deformation was exhibited in the as-deposited films, and no deformation was seen in detectors either before or after annealing. Test films of Bi-Te and Bi-Sb-Te were deposited onto thin glass substrates. Inductively coupled plasma spectroscopy indicated film compositions of $Bi_{20}Te_{30}$ and $Bi_{0.55}Sb_{1.45}Te_{36}$. After annealing at 300 “C in flowing argon gas for 2 h, the Bi-Te film exhibited a resistivity of 1.3x 10^{-5} Ωm and a Seebeck coefficient of -136 μV/K at room temperature. The annealed Bi-Sb-Te film had a resistivity of 2.2x 10-S Ωm and a Seebeck coefficient of 153 μV/K at room temperature.

Figs. 1 and 2 are schematic diagrams of a single detector pixel. Silicon wafers, three inches in diameter, 400 μm thick and (100) oriented were coated with 130 nm of low stress silicon nitride by chemical-vapor-deposition (CVD). A lift-off stencil was defined with an AZ 5214 photoresist [22] reversal process. Contact pads, to connect the two thermoelectric layers to each other and to a gold interconnect layer, were formed by lifting off 10 nm of gold over 40 nm of titanium. The gold interconnect layer, with a thin titanium adhesion layer, was then deposited and lifted off using a similar photoresist stencil. Thicker AZ 521 S photoresist stencils were used for the two 1 μm thick thermoelectric materials, which were deposited at ambient temperature and lifted off in acetone. Each detector has 11 thermocouple elements with 3 μm line widths. A 500 nm thick layer of silicon nitride was then deposited over the wafer in an electron-cyclotron-resonance (ECR) system with a substrate temperature of about 200 “C.

The silicon substrate was then removed under each array from the back side of the wafer with a hot potassium hydroxide etch. First etch windows were cut through the silicon nitride on the wafer back with a CF_4-O_2 reactive ion etch. The wafer was then placed face clown on a stainless steel plate and sealed around the edges with wax. The wafer and plate were placed in an etching jig with an o-ring seal around the wafer edge. Thus, the front side of the wafer was protected from the hot KOH etch by a double barrier of the o-ring and the wax. The wafer was etched for about 30 h in a 55 ‘C KOH etching solution composed of 440 g dissolved KOH pellets per liter of water. The wafer was then removed from the stainless steel plate with solvents.

One additional photolithography step was performed in order to open slits through the silicon nitride to separate the individual detectors in the arrays. Although the membranes are somewhat fragile, photoresist can be spun on using a vacuumless chuck. The slits through the silicon nitride membranes were cut with a CF_4-O_2 reactive ion etch. Photoresist removal after this etch is difficult, as ultrasonic cleaning or agitation in a solvent will break the membranes. Adequate photoresist removal can usually be achieved with a short oxygen plasma treatment followed by an acetone soak. Although a longer oxygen plasma exposure will remove the photoresist completely, this procedure can damage some thermoelectric materials. An absorbing layer of platinum about 40 Å thick was deposited on the back side of the wafer and membranes. The platinum thickness is determined by achieving a resistance of 160 to 200 Ω per square on a glass substrate placed next to the silicon wafer in the deposition chamber. Finally, the wafer was annealed in flowing argon at 300 “C for 2 h to improve the thermoelectric materials. Arrays were separated by cleaving along etched grooves.

Fig. 3 shows a section of a completed thermopile array. The 71 μm wide, 1.5 mm long, and 0.6 μm thick silicon nitride membranes are connected to the substrate only at their ends (right and left sides of picture). Horizontal 4 μm gaps separate the detectors. One side of each detector is connected electrically to a common electrode, shown across the left side of the photograph. Also included on the three inch wafer are chips with test structures to determine the electrical resistivities of the various metal layers and resistance of the contacts between the metals.

The most risky steps in the process are the back side KOH etch and the separation of the wafer from the stainless steel plate following this etch. If any membranes break during the etch, the KOH solution can leak to the front of the wafer and damage the thermoelectric lines through pin-holes in the passivating silicon nitride. In addition, usually a few membranes will break during separation. An alternate etching scheme would be desirable.

111. CHARACTERIZATION PROCEDURE

Four measurements on each detector determine the infrared responsivity, the response to electrical heating (electrical responsivity), the Seebeck coefficient of the thermocouples, and the detector response time. From these four measurements, one can additionally calculate the absorptivity, the effective pixel heat capacity, and the magnitude of the thermal conductance from the membrane. The thermal conductance is the sum of the conductance to the substrate through the silicon nitride membrane and thermoelectric materials plus the conductance due to radiative exchange with the environment.

Detectors are tested in vacuum. The zero frequency infrared responsivity is measured with a 1000 K laboratory blackbody. The response time for the 99 ms detectors described here is measured by recording the signal decay after a shutter in front of the blackbody is closed. For faster detectors, in which the 10 ms shutter speed is a significant fraction of the detector response time, the decay after an electrical heating pulse is recorded. The decays are approximately exponential out to at least twice the response time.

The detector electrical responsivity and Seebeck coefficient are measured using the circuit shown in Fig. 4. A square wave generator operating at about 0.3 Hz applies a -10 to O V signal to the base of a MOSFET switch pair. The switches connect and disconnect a battery voltage across the thermopile detector being tested. The current through the detector and the voltage across the detector are measured with battery-powered meters. An EG&G Princeton Applied Research 113 preamplifier [23] amplifies the signal, which is stored and averaged with a digital oscilloscope.

The current through the detector from the battery produces two thermal effects. Joule heating occurs along the lengths of the thermoelectric lines, and Peltier cooling or heating occurs at

the junctions between the two materials. The direction of current is such that Peltier cooling rather than heating occurs on the membrane. We make the simplifying assumption that the resulting temperature change in the central membrane area, as measured by the thermocouples, is the result of one half of the Joule heat generated plus all of the Peltier cooling at the thermally isolated junctions. It is assumed that the substrate is a good thermal ground and therefore any temperature change due to Peltier heat produced at the thermally grounded junctions is negligible. The heating power at the isolated junctions is therefore

$$H = IV/2 - INST. \qquad (1)$$

Here I is the current through the detector, V is the voltage across the detector, N is the number of thermocouples in each detector, S is the Seebeck coefficient of one thermocouple, and T is the substrate temperature. For small values of applied current the Peltier term dominates and the current acts to decrease the membrane temperature. As the current increases, the Joule heating term becomes dominant. The oscilloscope records a trace each time the current is removed from the detector. Immediately after the current is removed, the detector begins to recover to the substrate temperature according to its thermal response time. In order to measure the Seebeck coefficient of the thermocouples, the current is adjusted until the Joule heating and Peltier cooling terms are equal, as evidenced by a flat trace on the oscilloscope after the current is removed (disregarding transient signals). In this case equation (1) is equal to zero and S= $V/2NT$. The electrical responsivity is measured by increasing the current through the detector to produce a temperature difference of about 20 K between the membrane and substrate. The electrical responsivity is the ratio of the measured voltage signal immediately after the current is turned off to the electrical heat applied (equation 1). 'I'he measured electrical responsivity is fairly constant over a wide range of applied current.

Using the measured values of infrared responsivity, electrical responsivity, and response time, one can calculate values of detector absorptivity, thermal conductance, and heat capacity. The infrared and electrical responsivity at zero frequency are given by

$$R_{IR} = \eta\beta NS/G \qquad (2)$$

and

$$R_{EL} = NS/G. \qquad (3)$$

Here η is the absorptivity of the pixel, β is the fill factor, and G is the thermal conductance. The absorptivity and the thermal conductance can then be calculated with the relationships $\eta = R_{IR}/\beta R_{EL}$ and $G = NS/R_{EI}$. The heat capacity is given by the response time multiplied by the thermal conductance. Thus many of the relevant electrical, optical, and thermal properties of the detectors can be measured or calculated without specialized test structures.

It is typical to assume that Johnson noise is the only significant noise source in thermoelectric detectors. In order the verify this assumption for our detectors, noise was measured carefully at room temperature in three devices selected arbitrarily from the same array. A cap was placed over the array chip package to minimize temperature drifts within the array field of view. The detector output was amplified with a chopper-stabilized TLC2654 operational amplifier [24] connected as a non-inverting amplifier with a gain of one thousand. The TLC2654 amplifier's input-referred voltage noise of about 45 $nV/Hz^{1/2}$ is higher than the typical detector noise of 26 $nV/Hz^{1/2}$. However, the excellent low frequency noise characteristics of this amplifier allowed the detector noise to be measured at 20 mHz. The amplifier contribution to total noise was characterized by first shorting the amplifier input to ground to obtain the amplifier voltage noise spectrum. A similar spectrum was recorded with a 620 $k\Omega$ resistor between the amplifier input and ground. This second spectrum is the root-mean-square sum of the amplifier voltage noise, the amplifier current noise multiplied by the resistance, and the Johnson noise of the 620 $k\Omega$ resistor. The amplifier current noise spectrum was then calculated from these two measurements. Then a noise spectrum was recorded with the detector across the amplifier input. From this total noise spectrum, a root-mean-square subtraction of the amplifier voltage noise and the amplifier current noise times the detector resistance yields the noise due to the detector.

IV. RESULTS AND DISCUSSION

Table 1 lists detector dimensions and measured performance parameters at room temperature. These values represent average values of all pixels in two 63-element arrays (the responsivity standard deviation is the average of the standard deviations for the two arrays). The dc infrared responsivity of 1100 V/W for radiation from a 1000 K blackbody source, combined with the

detector resistance of 40,000 Q, gives a D*(f=O, 1000 K) value of 1.4x 10') cmHz$^{1/2}$/W. The average response time of the pixels is 99 ms.

Fig. 5 shows the total input-referred voltage-noise spectral density measured at the amplifier output with a thermopile detector across the amplifier input (short-dashed line). This total noise is about 50-55 nV/Hz$^{1/2}$ between 0.1 and 10 Hz. Also shown is the calculated detector noise (solid line). The detector noise was calculated using the amplifier characteristics, and was found to agree well with the calculated value of detector Johnson noise down to 20 mHz. For the three detectors tested, the average noise from 20 mHz to 10 Hz ranged from 26 to 28 nV/Hz$^{1/2}$, compared to the calculated Johnson noise of 26 nV/Hz$^{1/2}$ for the 42 Ω detector resistance. Temperature fluctuation noise for these detectors is expected to be about 6 nV/Hz$^{1/2}$ ($=2k_B^{1/2}NST/G^{1/2}$, with k_B being the Boltzmann constant), which contributes only a few percent to the total noise.

In order to compare these results with other thermopile detectors having different areas and response times, it is useful to use the figure of merit M_2 proposed by Jones [25,26]. Jones showed that for both bolometers and thermopiles, changing the geometry of a device results in changes in D^* and response time, τ, that are related by $D^*/\tau^{1/2}$ equal to a constant. The figure of merit M_2 is defined as M_2 = (6x10-" Ws/cm)·$D^*/\tau^{1/2}$. We have observed an approximately constant value of M_2 for a variety of device geometries on a single wafer, spanning about a factor of 12 in area and a factor of 6 in response time. The Bi-Te/Bi-Sb-Te thermopile arrays reported here have an M_2 value of 0.27, which is a factor of at least 3.5 higher than that of other reported values for thermopile arrays.

For many applications it is desirable for the detector responsivity and response time to have a small temperature dependence. Figs. 6 and 7 show the responsivity and response time for three detectors in the same array as a function of substrate temperature. In this particular array, the detectors are somewhat more responsive and faster than the averages shown in Table 1. Over the range 100-300 K the total change in each of these properties is about 20%. The detector resistance decreases by about 34% with decreasing temperature over the same range. The weak temperature dependence of the responsivity and response time are due to a balance between changes in thermal and electrical properties with temperature. As the detector temperature is decreased, the membrane

REFERENCES

[1] R. A. Wood, ''Uncoiled thermal imaging with monolithic silicon focal planes", *Proc. SPIE Vol. 2020, infrared Technology XIX*, 1993, pp. 322-329.

[2] C. Hanson, ''Uncoiled thermal imaging at Texas Instruments", *Proc. SPIE Vol. 2020, Infrared Technology XIX*, ,1993, pp. 330-339.

[3] P. M. Same, H. Yashiro, A. W. v. Herwaarden and S. Middelhoek, `` An Integrated Thermal Infrared Sensing Array", Sensors *and Actuators*, vol.14, pp. 191-201,1988.

[4] I. H. Choiand K. D. Wise, "A Silicon-Thermopile-Based Infrared Sensing Array for Use in Automated Manufacturing", *IEEE Transactions on Electron Devices,* vol. ED-33, pp. 72-79, Jan. 1986.

[5] W. G. Baer, K. Najafi, K. D. Wise and R. S. Toth, "A 32-element micromachined thermal imager with on-chip multiplexing", *Sensors and Actuators A,* vol. *48,* pp. *47-54, 1995.*

[6] T. Kanno, M. Saga, S. Matsumoto, M. Uchida, N. Tsukamoto, A. Tanaka, S. Itoh, A. Nakazato, T. Endoh, S. Tohyama, Y. Yamamoto, S. Murashima, N. Fujimoto, and N. Teranishi, "Uncooled infrared focal plane array having 128x128 thermopile detector elements", ***Proc. SPIE Vol. 2269, Infrared Technology XX*** , 1994, pp. 450-459.

[7] A. W. van Herwaarden, "The Seebeck Effect in Silicon ICs", *Sensors and Actuators,* vol. *6, pp. 245-254, 1984.*

[8] R. Lenggenhager, H. Baltes, J. Peer and M. Forster, "Thermoelectric Infrared Sensors by CMOS Technology", *IEEE Electron Device Letters*, vol. 13, pp. 454-456, Sept. 1992.

[9] M. von Arx, O. Paul, and H. Baltes, "Test Structures to Measure the Seebeck Coefficient of CMOS IC Polysilicon", *Proceedings of the 1996 IEEE International Conference on Microelectronic Test Structures,* vol. *9,* March 1996, pp. 117-122.

[10] R. Lenggenhagger, H. Baltes and T. Elbel, "Thermoelectric infrared sensors in CMOS technology", *Sensors and Actuators A, vol. 37-38,* pp. 216-220, 1993.

[11] D. F. Hornig and B. J. O'Keefe, "The Design of Fast Thermopiles and the Ultimate Sensitivity of Thermal Detectors", *The Review of Scientific Instruments*, vol. 18, pp. 474-482, July 1947.

becomes more thermally isolated as the silicon nitride thermal conductivity and radiative heat loss both decrease. Decreases in the thermocouple Seebeck coefficient and silicon nitride specific heat with decreasing temperature roughly balance out these effects, resulting in a fairly constant responsivity and response time. If the detector size is reduced, radiation effects become a small fraction of the total thermal losses. The temperature dependence of the thermal isolation in smaller detectors is thus dominated by the more slowly varying silicon nitride thermal conductivity. As a result, both the responsivity and response time of smaller detectors increase more dramatically with decreasing temperature.

V. SUMMARY

We have demonstrated the highest performance reported to date for an array of thermopile detectors. At room temperature detectors in 63-element linear arrays exhibit response times of 99 ms, zero frequency D^* values of 1.4x 10^9 cmHz$^{1/2}$/W and responsivity values of 1100 V/W when viewing a 1000 K blackbody source. The only measured source of noise above 20 mHz is Johnson noise from the detector resistance. Such arrays are well suited for uncooled dispersive point spectrometers.

ACKNOWLEDGMENTS

The authors are grateful to several people who assisted in this work. Professor Tom Kenny of the Mechanical Engineering Department at Stanford University supplied the CVD silicon nitride films. Roger Williams and Adam Kisor helped set up and test the sputter deposition system. Gary Plett provided the ICP analysis and Tom Hill operated the hot press for target fabrication. The authors benefited from discussions with Paul Kruse, Tim Krabach, Tom Van Zandt and Jean-Pierre Fleurial.

[12] R. A. Wood, T. M. Rezachek, P. W. Kruse and R. N. Schmidt, "IR SnapShot™ Camera", *Proc. SPIE Vol. 2552, Infrared Technology XXI, 1995, pp. 654-660.*

[13] M. L. Wilson, D. Kubisiak, R. A. Wood, J. A. Ridley and M. Listvan, "An Uncooled Thermo-Electric Microthermopile Camera Developed Using Silicon Microstructure Detectors", *Proc. IRIS Specialty Group on Infrared Detectors, vol.* 11, 13-16, August 1991, pp. 215-225.

[14] R. A. Wood, private communication.

[15] E. Ando, "Radiation Thermocouples with $(Bi,Sb)_2(Te,Se)_3$", *Japanese Journal of Applied Physics,* vol. 13, pp. 863-869, May 1974.

[16] R. Fettig, M. Balzer, U. Birkholz, J. Hofmann and H. Meyer, "Thermoelectric IR-Detectors", *Proceedings of the Eighth International Conference on Thermoelectric Energy Conversion and the Second European Conference on Thermoelectric,* July 1989, pp. 220-223.

[17] F. Völklein, A. Wiegand and V. Baier, "High-sensitivity radiation thermopiles made of Bi-Sb-Te films", *Sensors and Actuators A, vol. 29,* pp. 87-91, 1991.

[18] E. Johnson, A. Bodkin and M. Groden, Ion Optics, Inc., Waltham, MA.

[19] Kurt J. Lesker Company, Clairton, PA.

[20] Target Materials, Inc., Columbus, OH.

[21] Getter Corporation of America, Cleveland, OH.

[22] Electronic Products Division, Hoechst Celanese Corporation, Somerville, NJ.

[23] EG&G Princeton Applied Research, Princeton, NJ.

[24] Texas Instruments, Dallas, TX.

[25] R. C. Jones, "Factors of Merit for Radiation Detectors", *Journal of the Optical Society of America*, vol. 39, pp. 344-356, May 1949.

[26] R. C. Jones, "A New Classification System for Radiation Detectors", *Journal of the Optical Society of America, vol. 39,* pp. 327-343, May 1949.

FIGURE CAPTIONS

Fig. 1. Schematic top view of a single detector pixel.

Fig. 2. Schematic cross section of a single detector pixel.

Fig. 3. Section of a thermopile infrared detector array. The 71 μm by 1.5 mm by 0.6 μm silicon nitride membranes are connected to the substrate only at their ends (right and left sides of photograph). Horizontal 4 μm gaps separate the detectors. The common electrode is shown across the left side of the photograph.

Fig. 4. Circuit used to measure electrical responsivity and Seebeck coefficient.

Fig. 5. Voltage-noise spectral density as a function of frequency for a 42 kΩ thermopile detector. The detector signal is amplified with a Texas Instruments TLC2654 chopper-stabilized operational amplifier. The short-dashed line is the total noise, measured at the amplifier output and referred to the input. The total noise is about 50-55 $nV/Hz^{1/2}$ between 0.1 and 10 Hz. The solid line represents the detector noise of about 26 $nV/Hz^{1/2}$ calculated by performing a root-mean-square subtraction of the amplifier noise from the total noise. The long-dashed line is the 26 $nV/Hz^{1/2}$ Johnson noise of a 42 kΩ resistor.

Fig. 6. Responsivity as a function of substrate temperature for three detectors in an array, showing only about 20% change over the temperature range 100-300 K.

Fig. 7. Response time as a function of substrate temperature for three detectors in an array, showing only about 20% change over the temperature range 100-300 K.

TABLE CAPTIONS

Table 1. Typical detector dimensions and measured performance parameters at room temperature.

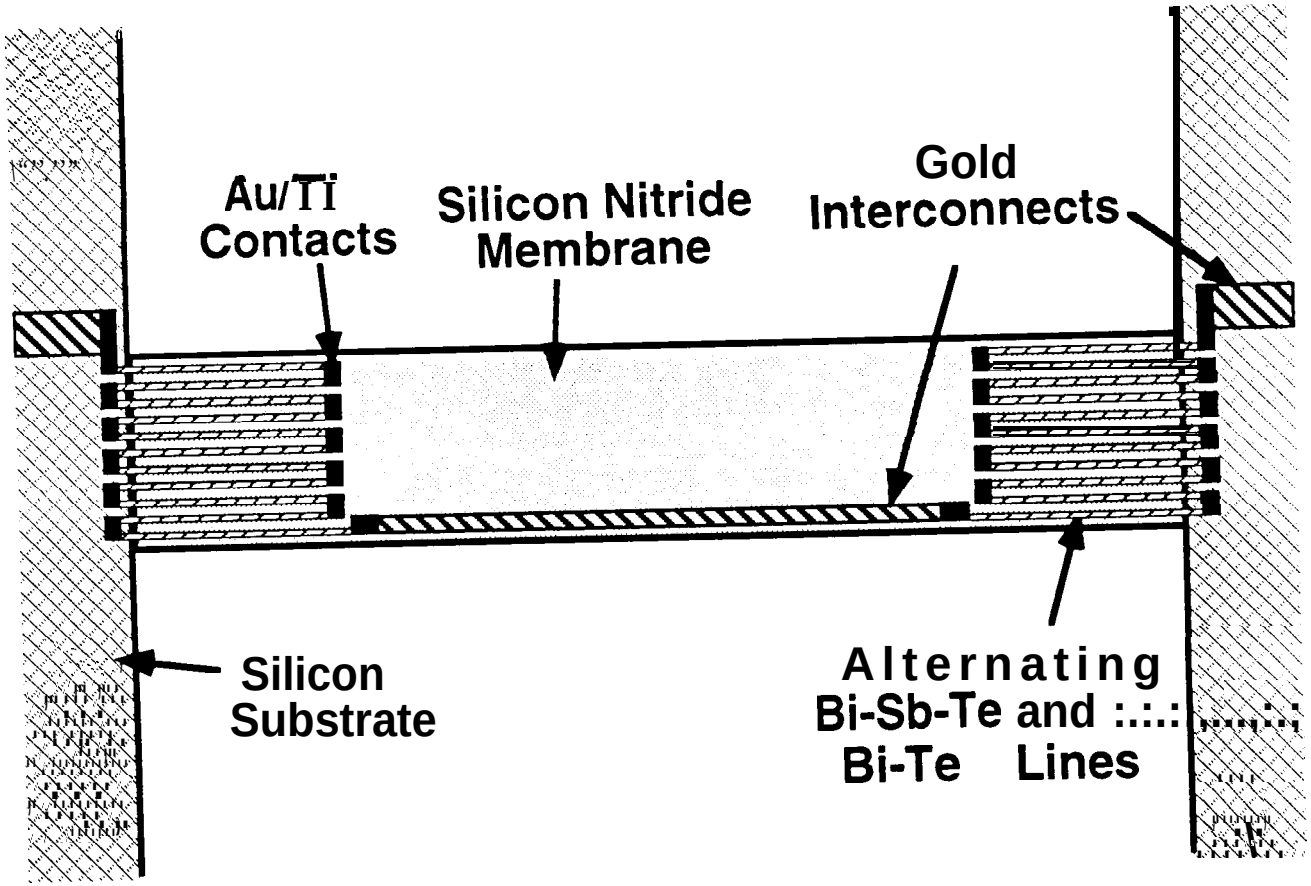
Au/Ti
Contacts
Silicon Nitride
Membrane
Gold
Interconnects
Silicon
Substrate
Alternating
Bi-Sb-Te and
Bi-Te Lines

Fig 1

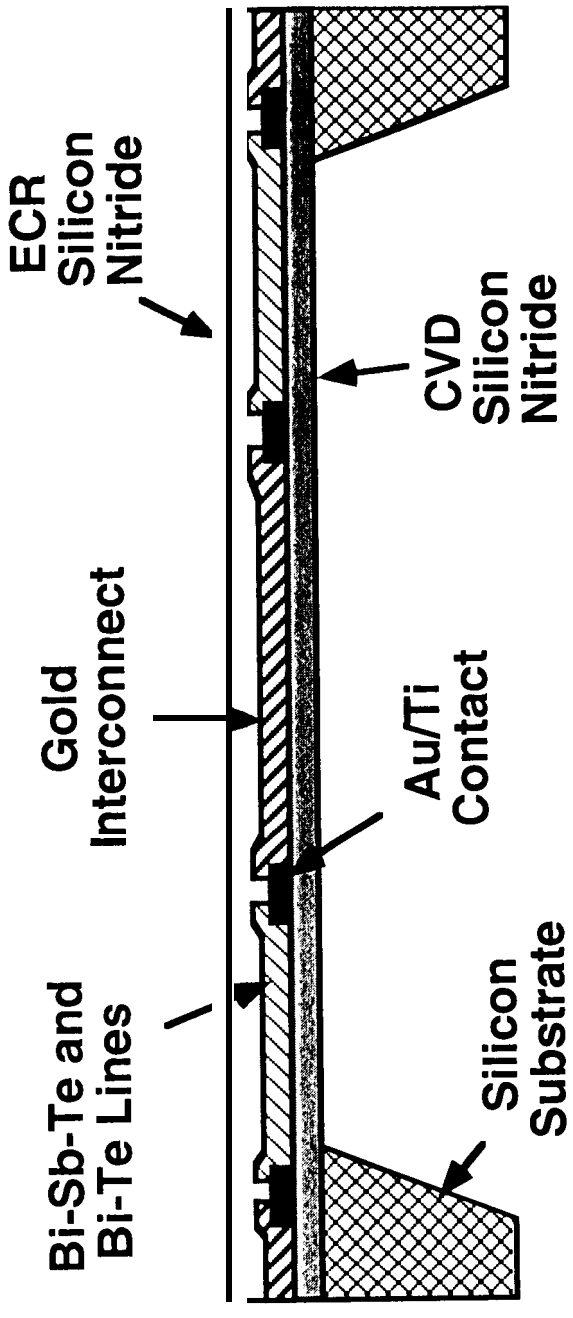
ECR
Silicon
Nitride
CVD
Silicon
Nitride
Gold
Interconnect
Au/Ti
Contact
Bi-Sb-Te and
Bi-Te Lines
Silicon
Substrate

Fig. 2

Current
Meter
Square Wave
Generator
Volt
Meter
Thermopile
Detector
Amplifier
Digital
Storage
Oscilloscope

Fig 4

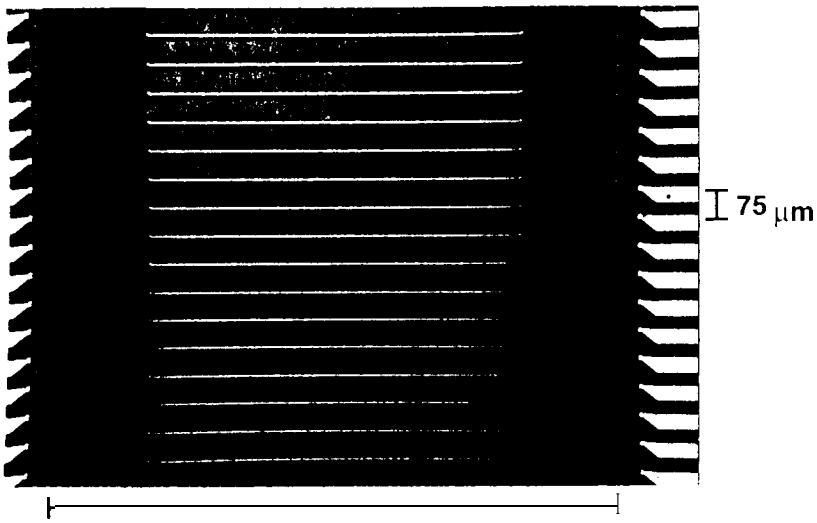

 Fig. 3

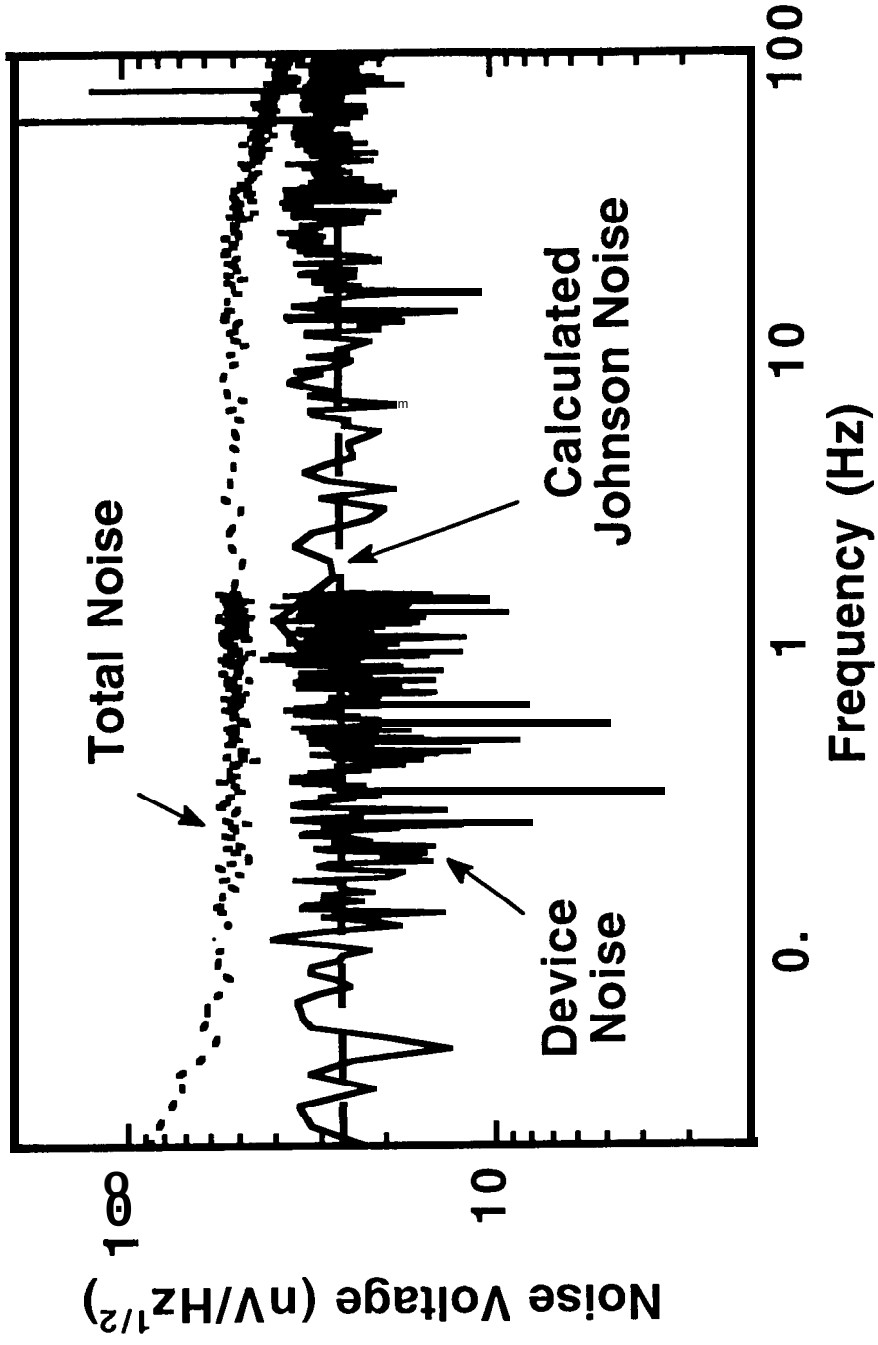
Noise Voltage (nV/Hz^1/2)
100
10
0.
1
10
100
Frequency (Hz)
Total Noise
Calculated
Johnson Noise
Device
Noise

Fig. 5

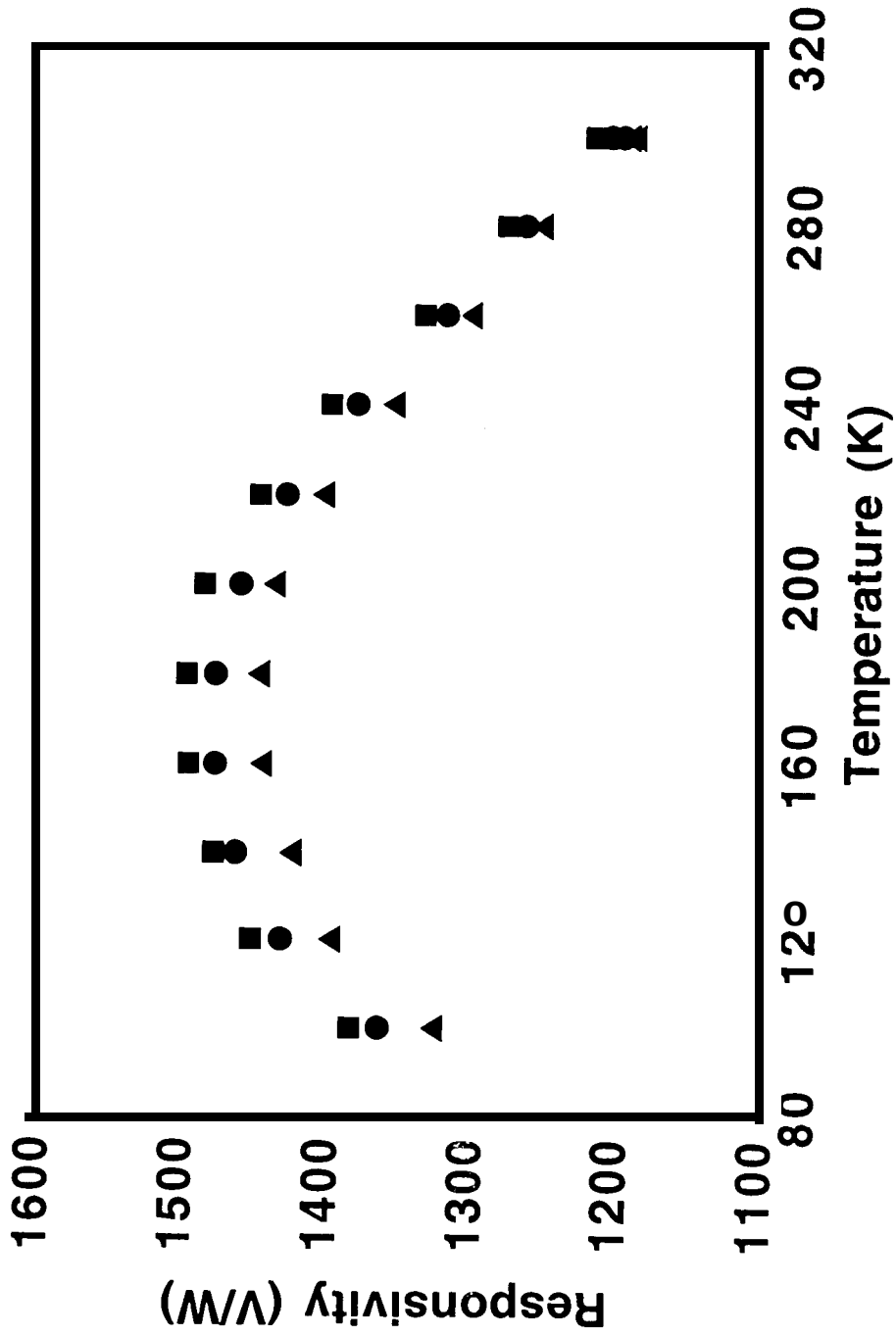
Responsivity (V/W)
1600
1500
1400
1300
1200
1100
80
120
160
200
240
280
320
Temperature (K)

Fig. 6

Parameter	Value
Detector Length (pm)	1,500
Detector Width (μm)	71
Pixel Spacing (μm)	*75*
Number of Thermocouples per Pixel	11
Seebeck Coefficient for one thermocouple (μV/K)	*300*
Resistance (Ω)	40,000
dc Infrared Responsivity (V/W)	1,100
Standard Deviation of Infrared Responsivity	±4.4%
dc Electrical Responsivity (V/W)	2,230
Response Time (ins)	99
D* (1000 K, O Hz) ($cmHz^{1/2}/W$)	1.4X1O'
Fill Factor	0.95
Absorptivity	*0.5*
Thermal Conductance (W/K)	I.5X10"^{6}
Heat Capacity (J/K)	1.5 X10-7

Table 1

120
110
100
90
80
Response Time (ms)
80
120
160
200
240
280
320
Temperature (K)

20

Fig. 7